Proceedings of the ASME 2018 37th International Conference on Ocean, Offshore and Arctic Engineering
OMAE2018
June 17–22, 2018, Madrid, Spain

OMAE2018-77703

ASSESSMENT OF EXPERIMENTAL UNCERTAINTY FOR A FLOATING WIND SEMISUBMERSIBLE UNDER HYDRODYNAMIC LOADING

Amy N. Robertson
National Renewable Energy Laboratory
Golden, CO, USA

Erin E. Bachynski
Norwegian University of Science and Technology
Trondheim, Norway

Sebastien Gueydon
Maritime Research Institute Netherlands
Wageningen, Netherlands

Fabian Wendt
National Renewable Energy Laboratory
Golden, CO, USA

Paul Schünemann
University of Rostock
Rostock, Germany

Jason Jonkman
National Renewable Energy Laboratory
Golden, CO, USA

ABSTRACT

The objective of this paper is to assess the sources of experimental uncertainty in an offshore wind validation campaign focused on better understanding the nonlinear hydrodynamic response behavior of a floating semisubmersible. The test specimen and conditions were simplified compared to other floating wind test campaigns to reduce potential sources of uncertainties and better focus on the hydrodynamic load attributes. Repeat tests were used to understand the repeatability of the test conditions and to assess the level of random uncertainty in the measurements. Attention was also given to understanding bias in all components of the test. The end goal of this work is to set uncertainty bounds on the response metrics of interest, which will be used in future work to evaluate the success of modeling tools in accurately calculating hydrodynamic loads and the associated motion responses of the system.

INTRODUCTION

Validation results from a test campaign of a semisubmersible floating wind system examined under the International Energy Agency (IEA) Wind Task 30, called the Offshore Code Comparison Collaboration Continued with Correlation (OC5) project, showed non-negligible underprediction of tower ultimate and fatigue loads by industry and research offshore wind modeling tools (see [1]). Differences were apparent for both wave-only and combined wind/wave load cases. For the wave-only cases, examination of the response spectral densities showed the largest differences between the experiment and simulation at the pitch natural frequency, which lies below the linear wave excitation region. However, the complexity of the system and test environment made it difficult to ascertain the cause of the underprediction. The differences could be related to the inability of the models to accurately represent the flow behavior and resulting hydrodynamic loads on the complex geometry of the structure. Or, it could be that the conditions of the test were not fully understood. In order to perform a successful validation, an uncertainty assessment of the test needs to be performed to set bounds on the level of certainty in the validation metrics. The test campaign examined in OC5 did not have the needed level of information available to perform an uncertainty assessment, which needs to be integrated in the initial planning stages of a validation project when a quantified validation is targeted.

The original test campaign examined within OC5 was performed by the DeepCwind consortium in 2013 at the Maritime Research Institute Netherlands (MARIN) offshore wave basin under combined wind and wave loading. In response to the outstanding questions found during the validation of this data, a follow-on test campaign was performed at MARIN (in the concept basin) under the MaRINET2 project with the same floating substructure, with a focus on better understanding the hydrodynamic loads and reducing uncertainty in the tests by minimizing complexity. The test matrix initially included examining the system in a constrained—as well as moored—configuration to better isolate individual hydrodynamic load components, but time constraints limited the testing to only the moored configuration. The goal of performing an uncertainty assessment of the test results was integrated in the planning of the test campaign. Repeat tests were performed for some of the load cases, and potential

sources of uncertainty were scrutinized throughout the planning, testing, and analysis stages.

The data from this test campaign is planned to be used within a future extension of the OC5 project to validate industry offshore wind modeling tools. The hope is that through an uncertainty assessment, as well as modeling the system with higher-fidelity modeling tools, the sources of the underprediction of the ultimate and fatigue loads seen during the OC5 project can be understood.

TEST SETUP

The structure that was tested in this campaign is the OC5-DeepCwind semisubmersible, which was previously examined under the OC5 project. FIGURE 1 - FIGURE 3 show the overall geometry and layout of the structure, and [1] provides the detailed geometric properties of the floater. The global coordinate system is defined with its origin at the center of the tower at the still water line. Positive X is then defined as downstream, Z is in the vertical direction, and Y is consistent with the right-hand rule.

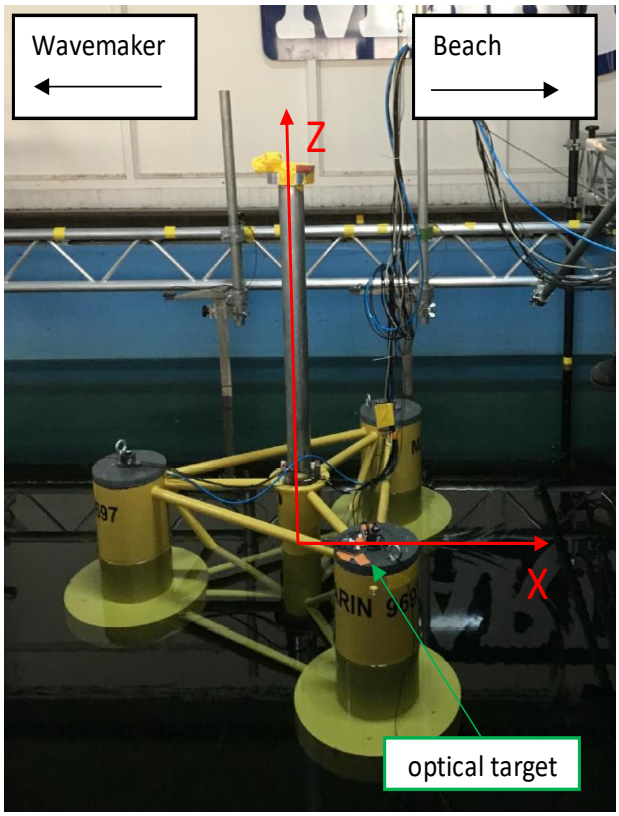

FIGURE 1: Test Setup (photo by Amy Robertson)

The same floating substructure was used in this test campaign as the one analyzed in OC5, but other aspects of the structure were simplified (see TABLE 1 for the main parameters of the model). No wind turbine was used since the focus was on the hydrodynamic response of the structure. Instead, a stout, rigid tower was implemented with some additional masses applied that approximately represented the overall mass and mass distributions of the OC5-DeepCwind semisubmersible. The mooring lines were also simplified to reduce uncertainty and fit in the narrow tank used for testing. Instead of a catenary configuration, taut angled lines were used that approximated the linear stiffness and initial vertical angle at the fairlead for the full catenary configuration. The mooring setup is shown in FIGURE 4 and includes a pulley at the bottom of the mooring lines connected to a spring of an appropriate stiffness, which is attached to a solid carriage system.

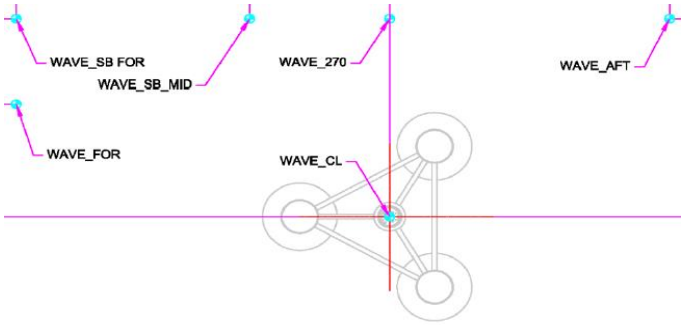

FIGURE 2: Location of wave probes in the tank

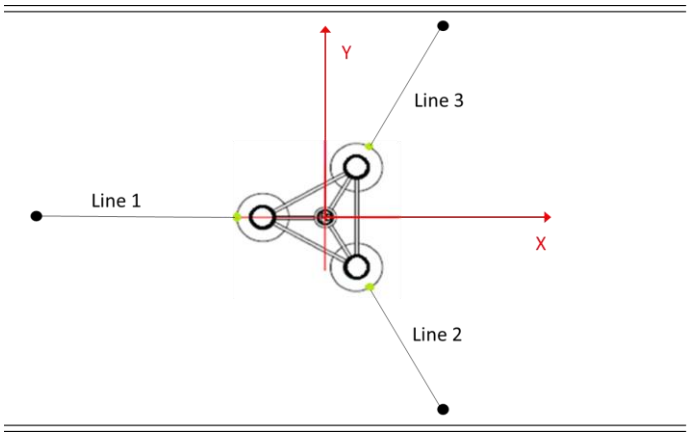

FIGURE 3: Location of anchors (pulleys)

The measurements performed during this test are as follows:

- Six degree of freedom (DOF) motions via optical system
- Three-by-three components of acceleration at the top of each of the outward columns
- Tension at the fairlead of the three moorings
- Wave elevations at five locations (six during wave calibration) – see FIGURE 2 for locations
- Wave maker flap position.

Unless otherwise noted, all information in this paper is presented at full scale, but the testing was performed at 1/50th scale.

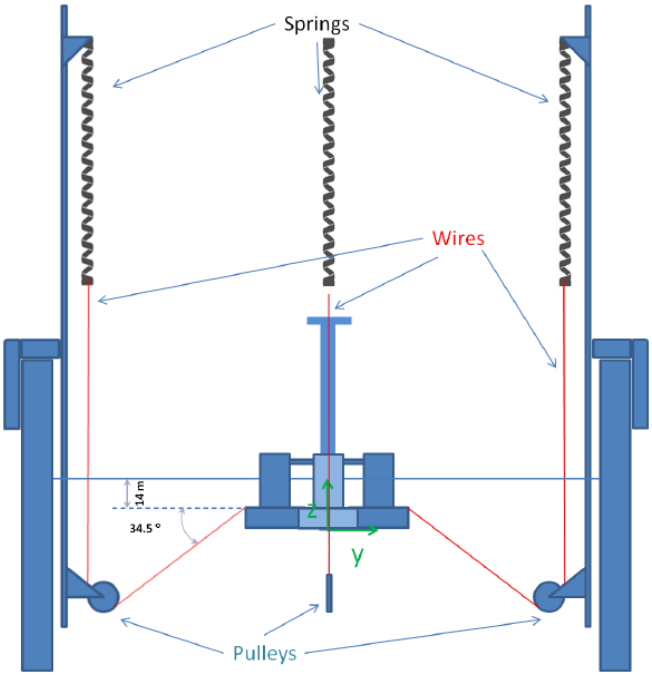

FIGURE 4: Taut-spring mooring line configuration

TABLE 1: Measured test specimen parameters. Desired pretension and mooring stiffness in parentheses. Anchor points are where the mooring line leaves the pulley.

Model mass	1.4196E+7	kg
Center of mass (CM)	[0, 0, -7.55]	[m,m,m]
X Moment of Inertia with respect to CM	1.29E+10	kg-m^2
Y Moment of Inertia with respect to CM	1.29E+10	kg-m^2
Z Moment of Inertia with respect to CM	1.42E+10	kg-m^2
Fairlead 1	[-40.87, 0.00, -14.00]	[m,m,m]
Fairlead 2	[20.43, 35.39, -14.00]	[m,m,m]
Fairlead 3	[20.43, -35.39, -14.00]	[m,m,m]
Anchor 1	[-105.47, 0.00, -58.40]	[m,m,m]
Anchor 2	[52.73, 91.34, -58.40]	[m,m,m]
Anchor 3	[52.73, -91.34, -58.40]	[m,m,m]
Mooring spring stiffness	48.9 (50.3)	kN/m
Mooring 1 pretension	1143 (1124.3)	kN
Mooring 2 pretension	1109.3 (1124.3)	kN
Mooring 3 pretension	1115.1 (1124.3)	kN

TABLE 2: Test matrix and natural frequencies. *The hammer test consisted of several hits in a single test, and the first five periods are reported. ** A sixth repetition was carried out, but with partially lost motion measurement.

Hammer and Decay Tests			
Description	**No. tests**	**Natural periods(s)**	
Surge decay	5	104.9	
Heave decay	5	17.33	
Pitch decay	5	31.17	
Roll decay	1	31.55	
Hammer test	1*	0.71, 0.50, 0.20, 0.15, 0.11	
Tests in Waves			
Wave	**Description**	**No. without model**	**No. with model**
Reg. wave 1	H=7.1 m, T=12.1 s	1	5
Reg. wave 2	H=4.0 m, T=9 s	1	2
Irreg. wave 1	H_s=7.1 m, T_p=12.1 s	1	5**
White noise	H_s=7.1 m, T=6-21 s	1	2

TEST MATRIX

The objective of this test was to better understand the response of the OC5-DeepCwind semisubmersible to hydrodynamic loading, especially the low-frequency responses in pitch and surge where second-order hydrodynamic loads can excite the pitch/surge natural frequencies. The end goal is to use the data to validate simulation models of the system.

To answer the objectives of the validation campaign, a series of tests were performed, as summarized in TABLE 2. To identify the hydrodynamic and structural properties of the test specimen, free-decay tests as well as a hammer test were performed. Repeat tests were done for the free decay to identify the variability in the response and the associated uncertainty in the hydrodynamic properties. The wave cases that were performed include two regular wave cases and two irregular conditions. Regular Wave 1 and the Irregular Wave cases were both repeated a total of five times over two days, whereas Regular Wave 2 and the White Noise Wave were each performed just two times. Repetition of the wave cases allows for an assessment of the randomness in the response of the system, which could stem from variation in the wave excitation, but also random behavior of the test specimen from unintended changes in the configuration and variability in the measurement devices.

UNCERTAINTY ASSESSMENT

To validate a simulation model against the measurements from this test, a set of response metrics are needed that represent the important physical quantities of interest [2]. The simulated value of the metric will never exactly match the measured one, so a range is needed on the measured value within which the simulated value would be considered acceptable. This data range is based on how certain the

measured value is. The metrics that will be used to assess the validation objectives for this test campaign are:

- Low-frequency response level–integral of power spectral density (PSD) over defined low-frequency range
- Mean drift offset
- Response amplitude operator (RAO) in surge, heave, and pitch at six discrete frequency points
- Ten highest response maxima for surge, heave, pitch, and mooring tension.

The goal of this paper is to define all of the uncertainty components that will be needed to determine the uncertainty bounds of these response metrics. The focus here is *experimental* uncertainty. Uncertainty in the numerical modeling is also an important topic for validation, and will be addressed in future work.

Several standards and guidelines are available that describe methods for assessing uncertainty in test campaigns. The International Standards Organization [3] and American Society of Mechanical Engineers [4] have developed standards that can be applied to any type of test. The International Towing Tank Conference (ITTC) has developed procedures and guidelines that provide more focused recommendations for assessing uncertainty in experimental hydrodynamics [5], seakeeping experiments [6], and offshore wind turbines [7]. Those who have started to address uncertainty for seakeeping tests have based their work largely on the recommendations presented in [8]. This publication is in Korean, but [9] provides a good summary of the methods presented by Yum, as well as a review of the work being done by others in this area.

Uncertainty in the response metrics from the experimental measurements will stem from uncertainties in the excitation of the system, the properties of the test specimen, and the accuracy and precision of the measurement equipment. All of these uncertainties need to be combined to estimate the overall uncertainty in the response metrics. However, for this paper, we focus only on identifying the individual component uncertainties, and future work will combine them to determine the response metric uncertainty bounds.

The sources of uncertainty are categorized using ASME terminology [4,10] as either random or systematic, with systematic uncertainties being those that create an unknown bias in the test, as opposed to randomly varying uncertainties that can be measured through repeat observations. We have attempted to appropriately label the uncertainties in such a manner in this paper, but these labels may need more evaluation.

Because repeat tests are available in this campaign, the random standard uncertainty of the response metrics, $s_{\bar{x}}$, can be evaluated directly as:

$$s_{\bar{x}} = \frac{s_x}{\sqrt{N}} \tag{1}$$

where s_x is the standard deviation of the response metric (x) across the repeated tests, divided by the square root of the number of observations (N). This valuation should assess the uncertainty associated with all random components of the experiment, including the excitation source, physical specimen, testing environment, and measurement sensors. However, in this paper, we have identified sources of random uncertainty in the individual components of the test as well (waves, test specimen, and so on)—where influences like the environment may cause the properties in the test to randomly vary. We have done this to get an overall view of where the largest uncertainty sources lie, and also in case some of the random components may be incorrectly categorized (i.e., they are actually systematic uncertainties).

The determination of the systematic uncertainty in the response metrics is not as straightforward as the determination of the random uncertainty. Because systematic uncertainty is something that creates an unknown bias in the measurement, it cannot be measured directly, and instead must be estimated. Each individual source of systematic uncertainty must be identified, including uncertainties associated with the excitation of the system, the test specimen properties, and the response measurement. These individual uncertainties must then be propagated to understand their effect on the uncertainty of the response metric, which can be accomplished using a simulation model. This paper again focuses only on identifying the individual uncertainty sources, and future work will propagate and combine them to determine an overall systematic standard uncertainty for each response metric.

Tables 3-5 (found in the Annex section) summarize all of the random and systematic uncertainty sources identified in this test campaign, which will be described in more detail in the following subsections. In general, “precision” is a term used to describe the variability of an instrument reading, and has therefore been categorized as a random uncertainty. On the other hand, accuracy is a description of the closeness between a measured value and a true value, and has therefore been categorized as a systematic uncertainty. Drift in a measurement can be seen when a nonzero value is measured when no excitation is present, and can fluctuate randomly or drift higher or lower as a result of nonrandom causes, such as a slow increase in air temperature in the room. In this paper, a mean change in a zero reading for a given sensor or across multiple sensors has been identified as a systematic uncertainty, whereas the variation of the value over a short period of time (e.g., oscillation of the measurement in one test before wave arrives) has been identified as a random uncertainty. Additionally, if a quantity is measured at only one or a few locations, but may vary spatially, the uncertainty in the value at a different location is classified as systematic.

Wave Excitation

For this test campaign, the primary excitation to the offshore wind structure is wave loading. Various aspects of the waves influence the hydrodynamic loading on the structure, including the wave elevation, velocities and accelerations, and their variation across the entire structure. However, only some

of these wave characteristics are measured in this test campaign. The time-varying wave elevation was measured at six locations, but the wave particle velocities, accelerations, and direction were not. Additional components influencing the hydrodynamic loading include the geometry and motions of the test specimen, possible water currents, water depth, and water density. A summary of the identified uncertainty values for the wave excitation are summarized in TABLE 3 and are discussed in the following paragraphs.

For the wave elevation measurement, the uncertainty is assessed using the full time series, rather than through properties, such as wave height and period, to better capture the influence of the individual wave trains. Sources of random uncertainty in the wave elevation have been identified as precision in the measurement instrumentation and variations in the environment. Wave probes were used to measure the wave elevation, and through calibration of the instrumentation, the precision was determined to be +/- 0.075 m. Variations in the temperature could affect the conductivity of the fresh water, which will alter the measurements of the resistance-type wave gauges used. A daily reading of the water temperature in the wave tank was taken, and values were recorded to vary between 17.2 and 17.6 ºC. Assuming perfect temperature measurements, this would result in an uncertainty of 0.8% in the measured wave elevations. Temperature variations will also influence the density of the water, which could affect both the draft and the wave loading on the model. However, the effect on water density is about 0.01% from this level of temperature change, and thus considered negligible.

Five repeat tests were performed for both Regular Wave 2 and the Irregular Wave cases. These repeat tests, as mentioned before, are another means for assessing the random uncertainty of the wave elevation time series, as the variability between individual measurements will be caused by the influence of all random uncertainty sources. The repeatability of the wave elevation is exemplified in FIGURE 5 and FIGURE 6. The time series of the wavemaker (WM) position is perfectly repeatable, and the time series of wave elevation shows generally good agreement in the primary wave frequencies. FIGURE 6 shows the 10 highest wave amplitudes from each of the repeated tests. The amplitudes are all within +/- 5% of the mean value (for each rank). For the highest wave amplitude of 10.5 m, the largest deviations are on the order of 0.3 m.

The sources of systematic uncertainty in the wave elevation are identified as error in the positioning of the wave probes and drift of the device, as well as three-dimensional (3-D) variation in the wave properties resulting from the influence of the tank boundaries. The potential uncertainty in the location of the wave probes was determined to be 0.25 m, and two degrees in tilt. Geometrically, this tilt gives an uncertainty of less than 0.001% on the wave elevation. The wave gauges were neither recalibrated nor zeroed after their initial calibration prior to the tests. As a result, the initial value of the wave elevation reading from each test is not exactly zero. This variation can be an indication of drift, temperature changes, changes in the water level in the basin, sagging or displacement of the trusswork that supports the wave gauges, or long seiching in the tank. The largest deviation observed in the wave elevation before waves arrived is 0.08 m. However, in the validation process, the wave input signals from the test campaign will be modified to have zero mean; thus, this offset will not contribute to the uncertainty. Instead, sensor drift was calculated based on the change in the mean value of the wave elevation over the course of one 3-hour wave test, which was found to be at most 0.03 m. As this uncertainty comes not only from sensor drift, but other sources as well, it has been identified as a systematic uncertainty.

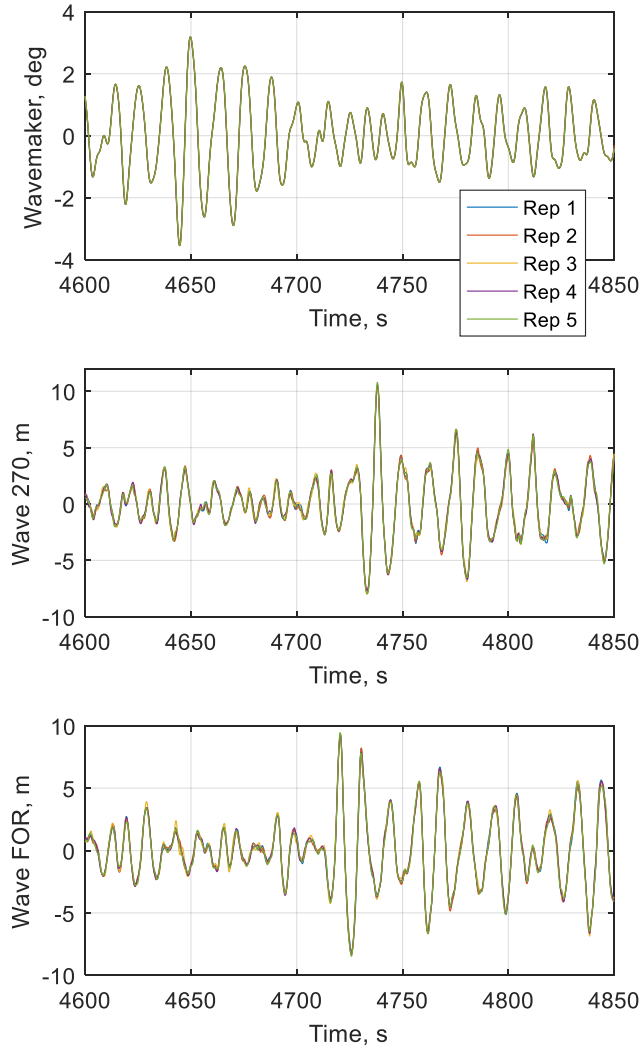

FIGURE 5: Repeatability of wave time series (Irregular Wave 1)

The influence of the tank boundaries can create the development of standing waves, such as sloshing or seiching, as well as reflections from the beach and side walls. The test specimen also radiates waves that reflect off the walls. These influences are captured in the measured wave *elevation*, but they may also influence the hydrodynamic *loads* on the model.

Reflected and standing waves, in particular, will contribute to the hydrodynamic loading, but these effects will not be captured by load models that assume that the measured wave elevation at these few points can be accurately represented by a long-crested wave train propagating from the wavemaker to the beach. Some of the spatial variation can be investigated by comparing the response of the system based on the wave elevation measured at different locations, but there are limitations to what can be assessed with the given measurement setup. As an example, in FIGURE 7 a subset of the time series for the Irregular Wave case is shown, where the measurement of the waves upstream of the structure (WAVE SB FOR) and beside that measurement (WAVE FOR), without the structure in the tank, are compared to the same measurements with the structure present. The differences in these measurements can be attributed to tank effects. A discussion of these tank effects is presented here, but quantification of these effects is mostly left for future work.

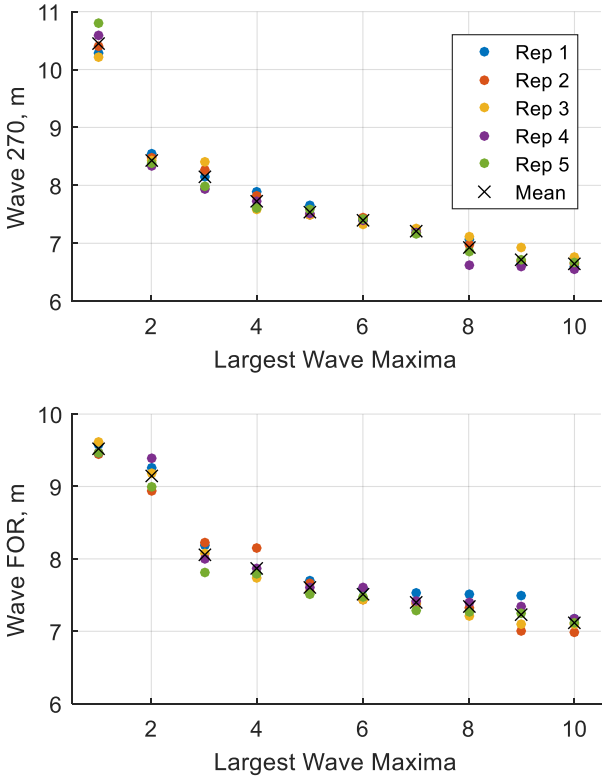

FIGURE 6: Repeatability of wave amplitude extrema, (Irregular Wave case)

Several of the test recordings continued long after the wave generation had stopped, and can provide some insight into the level of interaction the standing waves and reflections have on the dominant wave excitation. The transverse wave components from the first and second transverse modes of the tank (at 0.062 and 0.089 Hz, respectively) tended to be difficult to distinguish from the incoming waves during the tests, but were clearly visible in the period after the waves. FIGURE 8 shows the frequency content of Regular Wave 2 (9-s wave) during the test (top) and after the waves have stopped (bottom). After the testing stopped, the second transverse mode is evident at 0.089 Hz. For these tests, the transverse standing waves may be more important than the longitudinal sloshing, even though the transverse waves are perpendicular to the primary propagating wave. Nonetheless, based on linear theory, the forces due to the transverse standing waves are estimated to contribute less than 1% to the loads compared to the primary wave of interest.

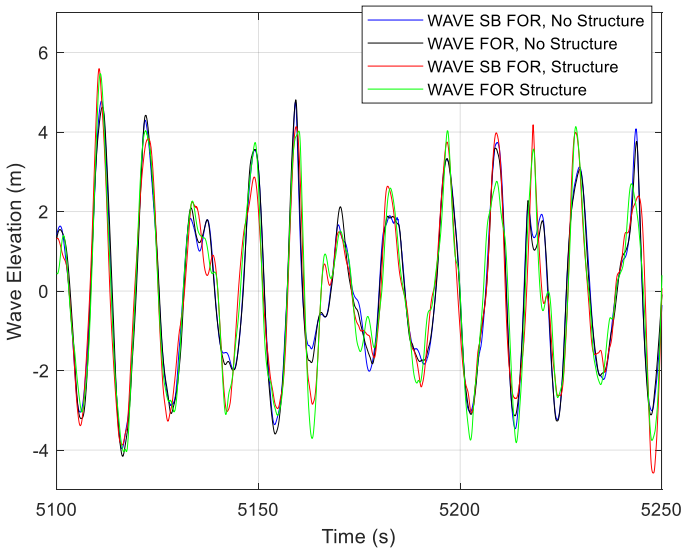

FIGURE 7: Variation of wave measurement based on location in the tank, and with structure present (Irregular Wave case)

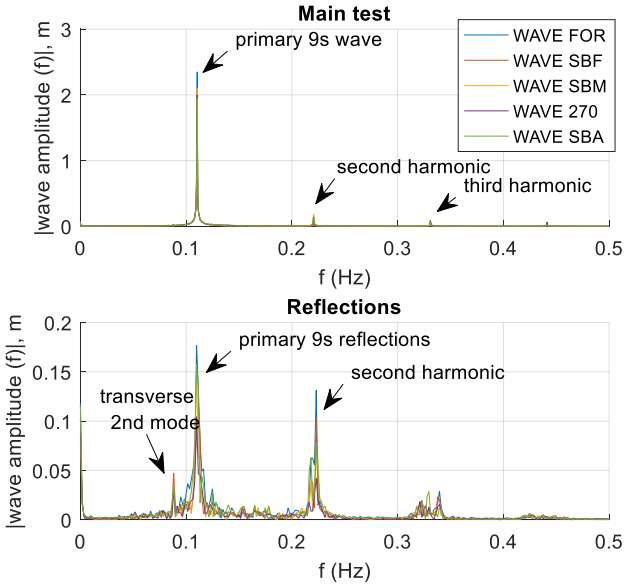

FIGURE 8: Wave elevation measurements during and after the Regular Wave 2 case

Even with a beach, it is impossible to completely avoid wave reflections in a tank of finite length. Examination of the

Regular Wave 2 case after the waves have stopped can enable some observations to be made on returning reflected waves. A time range of 600 s is used for this study, starting after the generated waves have passed the model and after the reflected waves have reached the model, but before the reflected waves have returned from the wavemaker. There is significant scatter among the wave gauges in this time period, which show wave amplitudes varying from 0.1 to 0.17 m at the 9-s frequency. This range of amplitudes would suggest a reflection coefficient between 5% and 8% for the given frequency. A similar analysis of the wave signals after the irregular wave was also carried out for five of the repeated tests. Here, the time range of interest was also taken to be 600 s, starting after the waves at 0.3 Hz would have reached the wave gauges. The standard deviation of the wave amplitude during this "reflection" period was 8%–9% of the standard deviation of the wave amplitude during the tests. Based on these observations, we may estimate the reflection coefficient in the tank to be on the order of 8%–10%. This factor includes the effects of the beach, but also includes some wave components that are reflected from the model back to the wavemaker, then again back to the model. Again, this study only provides an assessment of the influence the reflected waves have on the measurements, it is difficult to estimate what effect this has on the uncertainty in the hydrodynamic loads.

An additional effect of the tank boundaries—one of the other sources of systematic uncertainty—could be the presence of a slow current at the bottom of the tank as the water circulates back toward the wavemaker. Such a current could alter the wave kinematics distributions, but because of the significant water depth (180 m) and tank length, it was deemed that the influence for this test would not be significant. A final component is the variation of the depth of the tank, both spatially and potentially in time if water were to evaporate. Multiple measurements of the wave tank depth were performed at different locations and on different days, with a variation level of 2 m. This uncertainty will be considered as a potential bias in the water depth.

Test Specimen

Next, the uncertainties associated with the properties of the test specimen itself are examined. Previous validation campaigns that used completely functioning scaled wind turbines, such as the original testing of the OC5-DeepCwind system, suffered from uncertainties in the stiffness properties of the flexible members and joints, the arrangement and friction properties of the catenary moorings, as well as the influence of the cable bundle on both mass and stiffness [1]. The present campaign attempted to simplify the test specimen to eliminate some of these issues, but assessing remaining uncertainties is an important component to understanding the response. The list of uncertainties for the test specimen are provided in TABLE 4 and discussed in detail in the following paragraphs.

To determine the mass of the test specimen, two sets of measurements were performed with two different scales. For one of the measurements, the complete cabling for the sensors was included, situated on one of the columns. For the other set of measurements, a portion of this cabling was held off the structure—the amount that was approximated to be hanging off during testing. The mean values of the measurements with these two approaches differed by 250 g at model scale (3.13E+04 kg full scale). However, neither of these cases exactly represented the true configuration of the system in the tank, with an unknown portion of the cable bundle sitting on the structure and contributing to the mass. Therefore, the total mass of the cable bundle was identified as a potential bias in the mass measurement. The hanging mass of the cable bundle was estimated to be about 350 g in model scale, and that value was doubled to be conservative, resulting in a potential bias of 8.75E+04 kg full scale. The random standard uncertainty of the mass measurement was calculated using the five repetitions performed with the cable bundle included, resulting in a value of 3.93E+03 kg.

The center of mass (CM) of the system was calculated through a swing test. Again, the cable bundle was included in this calculation—placed on one of the offset columns. This calculation was repeated 10 times, with a random standard uncertainty of 4.3E-03 m in the z-direction at full scale (x and y variations were negligible). The system was built to have zero offset in the x- and y-directions, but a mean offset of 0.07 m in the negative x-direction was measured. The cable bundle could contribute to this offset as it was placed on one of the columns, but the mass was positioned in the positive x-direction, meaning that it was negating a potentially larger negative x-offset for the CM. The cable bundle was situated on a column that was also offset in the y-direction, so there is uncertainty in the CM in the y-direction as well. The influence of the cable bundle on the system CM was estimated to be 0.21 m (at full scale), and was assigned as a potential bias in both the x- and y-directions. The potential effect on the z-component of the CM was similar: 0.2 m. An additional source of uncertainty in the CM comes from weights that were added around the base of the tower to achieve a zero-offset initial configuration in the tank (see FIGURE 9). These weights were re-positioned in between the CM measurement and the actual testing. However, their influence was found to be considerably smaller than the influence of the cable bundle (as they are located much closer to the center of the structure), and therefore are not included in the uncertainty assessment. The accuracy of the CM measurement, estimated at 0.05 m, is small in comparison to the influence of the cable bundle, but still significant enough to include.

The inertia of the system was determined through the same swing test used for the CM. The random standard uncertainty across the 10 repetitions is reported in the random column in TABLE 4 for the x-, y-, and z-directions. Again, the influence of the cable bundle was assessed, and is placed in the systematic uncertainty column in TABLE 4, along with the impact of the accuracy of the measurement system (1%), and the influence of re-positioning the additional masses at the base of the tower. The configuration uncertainties are less important here than for

the CM, with the accuracy of the measurement instrumentation governing the uncertainty range.

The geometry of the structure is another source of uncertainty that can affect its hydrodynamic loading. Using expert opinion, a value of 2-mm uncertainty in the geometric dimensions was assigned (0.1 m full scale), impacting both the draft of the structure and diameter of the columns, as well as a 0.5-degree uncertainty in the angles of the individual columns, which are assumed to have no offset. In addition, changes in the initial position and orientation of the system can indicate changes in the system configuration (such as a change in draft), which could affect the system response. During many testing campaigns, the measured initial position of the structure is zeroed at the beginning of every test, erasing this valuable information. For this test campaign, the initial position was only zeroed at the beginning of the first test (and no others), thus providing the initial conditions for each individual test. These measurements can be used to alter the system properties in a way that creates a similar neutral position/orientation. However, the cause for the offset could be difficult to determine and therefore how to appropriately adjust the system properties. For instance, a change in heave position could indicate that the system has taken on water, or it could indicate that the mooring lines have changed their positioning. Across all of the tests, the maximum differences in the neutral position of the structure between the beginning and end of the test were 0.12 m in translation, and 0.062 degrees in rotation.

FIGURE 9: Additional weights (red) placed around the foot of tower (photo by Sebastien Gueydon)

Uncertainty in the stiffness of the individual members and joints was seen to add considerable uncertainty to previous test campaigns. For this test, the system was attempted to be made as rigid as possible. No wind turbine was present, and a rigid, rather than flexible, tower was used, but there may still be some level of flexibility in the system. Accelerometers were placed on each of the offset columns of the structure to assess whether there are any relative (nonrigid body) motions occurring between the individual columns. A comprehensive analysis of the accelerations has not yet been completed, but initial examination indicates that flexibility of the members will not contribute significantly to the uncertainty in these tests.

The mooring behavior was also a significant source of uncertainty for previous test campaigns, which was reduced here by having a shortened, taut configuration rather than a catenary system (with the potential for significant uncertainty in the layout of the moorings and the friction contact with the seabed). Uncertainty is still present, though, in the properties of the moorings (mass, stiffness, damping), the initial preload in each line, as well as the positions of the fairleads and anchors. The stiffness of the lines has the most influence on the quantities of interest here—the measured tensions and the influence of the moorings on the system response—and the uncertainties related to the mass and damping are considered negligible in comparison. The mooring configuration is shown in FIGURE 4 and consists of the three individual wires that are run through pulleys at the fairlead location and then connected to springs positioned vertically above the pulleys. The wires themselves do not stretch, and the tension in the lines comes from the springs. The spring specifications stated a stiffness of 50.3 kN/m (full scale), but stretch tests of the springs put this value at around 48.9 kN/m, with a 0.2% variation between individual springs. Offset tests in the tank showed a mean value of 47.4 kN/m, with a 5% variation between individual lines. The differences between these individual measurements/ prescriptions were used to assign an overall uncertainty in the tension properties of 5.2 kN/m, or about 10% (difference between prescribed and smallest value calculated was 45.1 kN/m). This mean variation will need to be considered as well as the potential for variation between the individual springs. The initial preload for the moorings is another important component, and the associated uncertainty was assessed by examining the differences observed in the measurements at the start of the tests before waves arrived. Significant differences were seen between the individual lines, and across different tests. There was a shift in the preload values between the first and second day of testing. No correlation was found to a shift in the position of the structure, and so it is unknown why the preload values would change significantly. In the end, a range of 362 kN was observed for the preload across all lines and tests. Finally, the angle and position of the moorings may affect the interaction they have with the structure, and the uncertainty in these properties is assigned through the precision of the fairlead and anchor positions, as shown in TABLE 4.

One final consideration is the roughness of the surface of the structure. To investigate this influence, simulations will be run in the future with multiple drag coefficients correlated to varying roughness values, to examine the effect on the response of the system.

Response

The final source of uncertainty in the experiment is from the measurements used to derive the response metrics, as well

as the processing of the data. Most important for the metrics of this test campaign are the motion measurement, mooring line tension, and wave elevation measurement (for estimating RAOs). The uncertainties in the wave elevation measurement are discussed in the Wave Excitation section. Accelerations were also measured, but these signals are mainly used to check the motion measurements and ensure that there is little relative motion between the individual columns of the semisubmersible, thus ensuring the structure is fairly rigid.

The uncertainty associated with the motion measurements includes uncertainties from the tank definition, camera, dimensions of the model target, measurement setup, and the measurement range for these specific tests (15-m surge displacement). The combination of all of these sources (which is placed in the systematic column but contains some random attributes as well) resulted in a final position uncertainty of 0.03 m (as shown in

TABLE 5). The corresponding angle uncertainty is 0.3 degrees. In addition, because measurements were available for the motion before and after the wave train arrived/passed the test specimen, this portion of the signal can be used to further examine potential uncertainty. The motion measurements were observed to oscillate (with no excitation) at a level of about 0.02 m in surge and 0.05 degrees in pitch (assigned as random uncertainty). A mean offset was also observed in these motion values without waves, but this could be a result of an actual shift in the initial position, and will be included as an initial condition for simulations.

FIGURE 10 shows an example of the repeatability of the motion responses, and FIGURE 11 shows the 10 maximum amplitudes of motion for the Irregular Wave condition. The deviation of any single repetition from the mean (for these 10 maxima) is less than 4% for surge and less than 5% for heave and pitch.

The tensions in the mooring lines were measured using ring load cells that have been manufactured by MARIN. For these tests, the expected tensions were small (pretension of 8.8 N at model scale), but the maximum range of the load cells was large. For small tension values, larger levels of uncertainty were present. Using a single value for the entire tension range, a value of 5% uncertainty in the tension value was deemed appropriate. Because the dynamic variation of the tension might be small, there is potential that the uncertainty may be larger than the 5% value. Similar to the motion measurements, the tension measurements during rest showed an oscillation magnitude of about 6 kN.

The processing of the measurements is another source of uncertainty, including the data conversion, time sampling, time averaging, time synchronization, and numerical precision of the data acquisition system, as well as the derivation of statistical properties from the data. These sources of uncertainty are typically fairly small, and are assumed to be insignificant compared to other sources of uncertainty for this test campaign.

SUMMARY

In this paper, the sources of uncertainty in a test campaign of a floating semisubmersible have been identified. The uncertainty in the wave elevation is dominated by the random uncertainty, with the repeatability of peaks typically being within 5%, and the estimated systematic errors contributing less than 0.01% for the same peaks. Despite the low uncertainty in the wave elevation, there may be more significant uncertainty in the wave loads (which were not measured directly) due to finite tank effects (especially reflections). This point will be examined in greater detail in future work. Even for a simple model, there are important uncertainties in the physical properties of the model itself. The uncertainty in the mass and in the center of mass is dominated by the measurement cable weight, whereas the uncertainty in the inertia is dominated by the accuracy of the measurement equipment. The measurement of motion responses is precise, while the tension measurements in the moorings were carried out with force gauges that were not entirely appropriate for the load levels—resulting in a high random uncertainty. The repeatability of the motion responses was similar to the repeatability of the wave elevation (within 5% for the peaks).

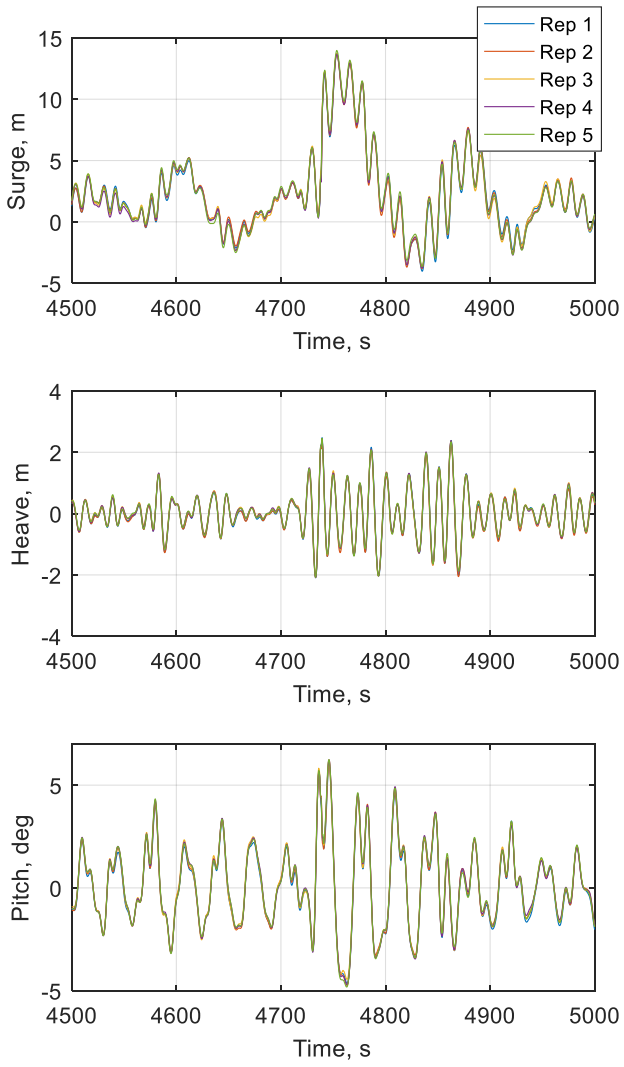

FIGURE 10: Repeatability of motions (Irregular Wave 1)

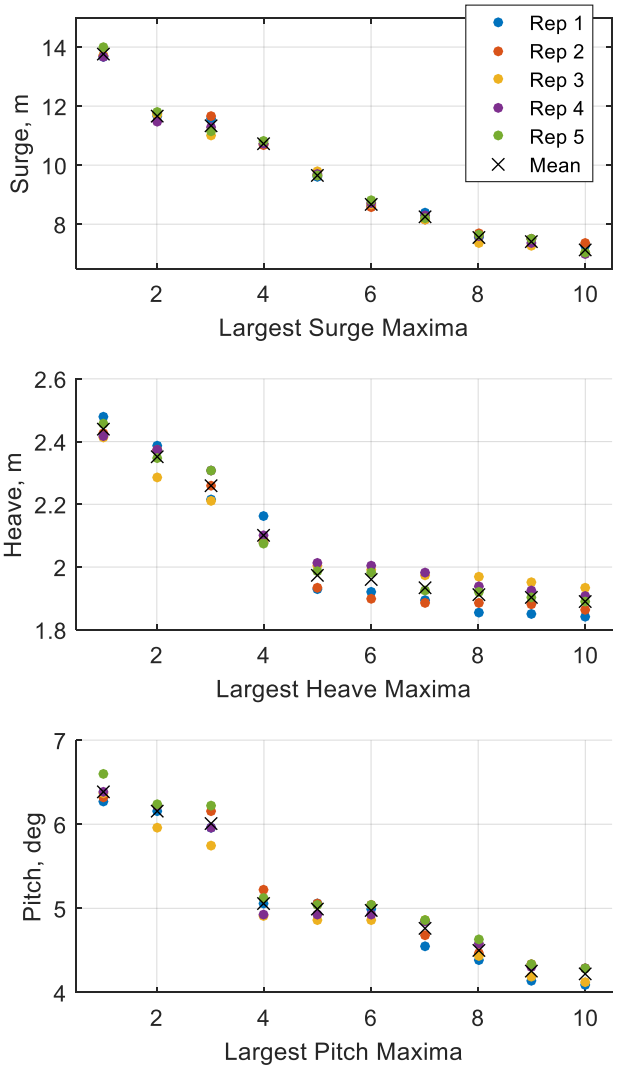

FIGURE 11: Repeatability of motion amplitude extrema (Irregular Wave 1)

The end goal is to combine each of these uncertainty sources in future work to determine the level of uncertainty in response metrics that will be used to validate simulation models of the test specimen. For the systematic uncertainty, sources from the wave excitation and specimen properties will need to be propagated to the uncertainty in the response of the system, which will be achieved through a simulation model. The random uncertainty levels in the response will be examined directly through the repeatability across multiple iterations of the same test as well as the precision of the instrumentation. The combination of the random and systematic uncertainties will enable an uncertainty range to be assigned for each response metric.

This work addresses one aspect of better understanding the reason for discrepancies seen between the test data and simulations in a previous validation campaign examined within the OC5 project. Additional work is needed to determine potential shortcomings of the present modeling approaches in research and industry design tools in capturing the hydrodynamic loading on the complex floating semisubmersible geometry. This will be accomplished in future work by testing the structure under constrained conditions—to better isolate the individual hydrodynamic load components on the structure, and through higher-fidelity modeling of the system—to understand where design tool capabilities break down.

This paper shows one of the first attempts to identify and calculate the level of uncertainty in a floating wind test campaign. Further work is needed to ensure all sources have been properly captured and to identify ways to further eliminate uncertainty in the test process. It is imperative that uncertainty

is addressed in future test campaigns from the planning stages to ensure that the proper information is captured to assess the bounds on the response behavior of interest. For validation, further work is also needed to understand sources of uncertainty/sensitivity in the modeling approaches being examined. By addressing both test and modeling uncertainty, designers and analysts will better understand how to use design tools effectively and assign confidence values to their performance/load estimates.

ACKNOWLEDGMENTS

The authors would like to acknowledge the support of the MARINET2 project (European Union's Horizon 2020 grant agreement 731084), which supplied the tank test time and some travel support to accomplish this validation campaign.

The work by the NREL authors was supported by the U.S. Department of Energy under Contract No. DE-AC36-08GO28308 with the National Renewable Energy Laboratory. Funding for the work was provided by the DOE Office of Energy Efficiency and Renewable Energy, Wind Energy Technologies Office.

The U.S. Government retains and the publisher, by accepting the article for publication, acknowledges that the U.S. Government retains a nonexclusive, paid-up, irrevocable, worldwide license to publish or reproduce the published form of this work, or allow others to do so, for U.S. Government purposes.

REFERENCES

[1] Robertson, A., et al. (2017). "OC5 Project Phase II: Validation of Global Loads of the DeepCwind Floating Semisubmersible Wind Turbine," *Energy Procedia*, Vol 137, pp. 38-57.

[2] Hills, R., Maniaci, D., Naughton, J. (2015). "V&V Framework," *SANDIA Report SAND2015-7455*.

[3] ISO (1993). "Guide to the Expression of Uncertainty in Measurement," International Standards Organization, Geneva, Switzerland.

[4] ASME (2013). "Test Uncertainty, Performance Test Codes," ASME PTC 19.1-2013.

[5] ITTC (2008a). "Guide to the Expression of Uncertainty in Experimental Hydrodynamics," Recommended Procedures and Guidelines, 7.5-01-01.

[6] ITTC (2008b). "Testing and Extrapolation Methods; Loads and Responses, Seakeeping; Seakeeping Experiments," Recommended Procedures and Guidelines 7.5-02-07-02.1.

[7] ITTC (2014). "Model Tests for Offshore Wind Turbines," Recommended Procedures and Guidelines 7.5-02-07-03.8.

[8] Yum, D. J., Lee, H. Y., and Lee, C. M. (1993). "Uncertainty analysis for seakeeping model tests," *J. Soc. Nav. Archit. Korea* 30 (3), 75-89.

[9] Kim, Y. and Hermansky, G. (2014). "Uncertainties in seakeeping analysis and related loads and response procedures," *Ocean Engineering*, 86, 68-81.

[10] Robertson, A. (2017); "Uncertainty Analysis of OC5-DeepCwind Floating Semisubmersible Offshore Wind Test Campaign," presented at *The International Society of Offshore and Polar Engineers Conference*, June 2017.

ANNEX

TABLE 3: Wave excitation uncertainties.

Parameters	Systematic Uncertainty		Random Uncertainty	
		Uncertainty		Uncertainty
Wave elevation (m)	Wave probe position error	<0.001% due to tilt	Repeat measurements at same location	Full time series
	3D variation – variation across sensors	Full time series	Wave probe measurement precision	0.075
	Sensor drift	0.03	Wave probe temperature effects	0.80%
			Variation before wave arrives	0.2
Water depth (m)	Run simulations at different depths	2.0		
Water density (kg/m^3)			Temperature effects	0.01%

TABLE 4: Test specimen uncertainties.

Parameters	Systematic Uncertainty		Random Uncertainty	
		Uncertainty		Uncertainty

Mass (kg)	Cable weight	8.75E+4	Standard Uncertainty:	3.95E+3
CM (m)	Location of additional masses		Standard uncertainty:	
	X	0.21	X	0.0
	Y	0.21	Y	0.0
	Z	0.20	Z	4.30E-3
	Accuracy (0.001 m model scale):			
	X	0.05		
	Y	0.05		
	Z	0.05		
Inertia (kg-m^2)	Accuracy (1%)		Standard uncertainty:	
	Ixx	1.26E+8	Ixx	1.87E+6
	Iyy	1.25E+8	Iyy	9.91E+5
	Izz	1.38E+8	Izz	5.69E+5
	Influence of cable bundle			
	Ixx	2.12E+5		
	Iyy	1.80E+5		
	Izz	1.00E+5		
	Location of masses at base			
	Ixx	8.00E+4		
	Iyy	8.00E+4		
	Izz	8.00E+4		
Geometry	Draft (m)	0.1		
	Column angle (degrees)	0.5		
	Column diameter (m)	0.1		
Initial position/orientation	Translation (m)	0.12		
	Rotation (˚)	0.062		
Moorings				
Stiffness (kN/m)	Difference in measurement vs. prescribed	5.2		
Mooring preload (kN)	Differences in initial values	362		
Mooring fairlead position (m)			Precision	0.05
Anchor position (m)			Precision	0.25
Roughness	Change drag coefficient	TBD		

TABLE 5: Response uncertainties.

Parameters	Systematic Uncertainty		Random Uncertainty	
		Uncertainty		**Uncertainty**
Motion measurement				
Translation (m)	Translational (m)	0.03	Observed variation before wave – trans. (m)	0.02
Rotation (degree)	Rotational (degree)	0.3	Observed variation before wave – rot. (˚)	0.05
Mooring tension measurement (N)			Precision	5.00%
			Observed level of variation before wave	6
Acceleration measurement (m/s^2)	Amount zero value differs between sensors	0.06	Observed level of variation before wave	0.025
	1 deg misalignment potential	1.70%	Precision	5.00%
Data acquisition system	Assume negligible			
Data conversion (volt/wave ht)				

Time sampling				
Time averaging				
Time synchronization (w/ opt)				
Numerical precision				
Data processing	Assume negligible			
Freq. analysis - # periods /sampling				